Reprinted from Proceedings of the 28th International Conference on Coastal Engineering, Cardiff, UK, pp. 705—717, 2002.

WAVE BREAKING AND RIP CURRENT CIRCULATION

Merrick C. Haller[1] and H. Tuba Özkan-Haller[2]

Abstract: This paper examines the effect of current-induced breaking on the modeling of wave breaking dissipation near rip currents. Simulations using a set of existing wave transformation models are compared to existing laboratory measurements made on a bar/channel topography in the presence of both strong and weak rip currents. The model/data comparisons demonstrate that existing models can effectively simulate the wave breaking near rips, but only by making large adjustments in the model coefficients used in the wave dissipation parameterizations. Since wave breaking formulations are typically calibrated without regard to the cross-shore currents, these results suggest that most model predictions will suffer large errors near rip currents. Furthermore, any errors in the modeled wave breaking dissipation will affect model predictions of the wave setup/setdown and, therefore, the wave driven circulation. A simple model exercise shows that predictions of the longshore pressure gradient, which is a driving force for the rip circulation cells, can be sensitive to the accurate simulation of wave breaking near rip currents.

INTRODUCTION

Rip currents are one of the more elusive features of the nearshore ocean; they are difficult to measure, difficult to model and predict. But despite their difficult aspects, it has been well established that, as with most nearshore motions, they are driven by wave breaking. In addition, since rip currents flow in the offshore direction, they can have a strong feedback on the incoming wave field.

Typically, shoaling and wave breaking in the nearshore is induced by the steady decrease in depth as waves approach the shore. However, the presence of an opposing current will also cause waves to shoal, steepen, and eventually break. For waves propagating on seaward flowing rip currents, it is highly likely that some combination of depth- and current-induced breaking occurs, and since rip currents tend to be very limited in their longshore extent, this implies that the dynamics of wave breaking can have strong variations in the longshore direction when rip circulations are present.

WAVE DISSIPATION MODELING

In order to model wave shoaling and breaking in the presence of opposing currents, it is convenient to use the wave action balance equation. In one horizontal dimension the wave action balance including dissipation is given by

1 Asst. Prof., Dept. of Civil, Constr., and Env. Eng., 202 Apperson Hall, Oregon State University, Corvallis, OR 97331-2302 USA. hallerm@engr.orst.edu.

2 Asst. Prof., College of Oceanic and Atmospheric Sciences, Oregon State University, Corvallis, OR, 97331-5503 USA. ozkan@coas.oregonstate.edu.

$$\frac{d}{dx}\left[\frac{E}{\sigma}(Cg+U)\right]=\frac{D}{\sigma} \quad , \tag{1}$$

where $E=\rho g H^2/8$ is the wave energy, H is the wave height, σ is the intrinsic wave frequency, C_g is the group velocity in a reference frame moving with the current (U), and D is the energy loss due to breaking. For our comparison we will utilize the following three models for wave breaking dissipation: 1) Battjes and Janssen (1978), which is based on dissipation in a turbulent bore, 2) Dally, Dean, and Dalrymple (1986), which is based on a "stable energy flux" criterion, and 3) Chawla and Kirby (2002), which is a recently introduced modification of the bore dissipation formulation that is intended to better simulate current-induced breaking. The modified bore dissipation model of Chawla and Kirby (CK) was derived for wave breaking on opposing currents in intermediate and deep waters, and in their model/data comparisons the opposing currents were strong and the waves were near the blocking point. Therefore, the CK model may be more appropriate when the rip current strength approaches the blocking condition. However, it is not presently known how often wave blocking by rip currents occurs.

Rip Currents and Wave Blocking

First it is of interest to investigate the importance of wave blocking by rip currents. The linear dispersion relation for waves propagating on a colinear current is given by the following:

$$(\omega - kU)^2 = gk\tanh(kh), \tag{2}$$

where ω is the absolute frequency relative to a stationary observer, k is the wavenumber, and h is the local water depth. Wave blocking occurs when the absolute group velocity is reduced to zero, i.e. $U+C_g = 0$. Using Eq. (2) and the following equation for Cg:

$$Cg = \frac{\sigma}{2k}\left(1+\frac{2kh}{\sinh 2kh}\right), \tag{3}$$

the ratio U/C_g can be calculated for a given wave frequency, rip current velocity, and water depth. This ratio is plotted in Figure 1 for a range of field-scale wave and current conditions. The chosen parameter values represent the conditions at the rip head (*i.e.* the rip current maximum) and span the expected range for field-scale rip currents.

If we consider incident wave periods to most often lie between $5 < T < 15$ sec and rip current velocities to be ~ 1 m/s, we can see from the figure that for h=1m the ratio U/Cg approaches 1.0 for only a fairly restricted range of wave periods and rip velocities (*i.e.* $T <$ 8 sec and $U>1.5$ m/s). As the water depth of the rip maximum increases, the conditions for wave blocking become even more restrictive. This suggests that wave blocking by rips should be fairly rare. However, it should also be noted that rip currents are commonly unsteady and any energetic pulses of ~ 0.5 m/s may induce wave blocking temporarily.

Experimental Data

There are relatively few data sets that effectively capture observations of wave dissipation near rip currents. To our knowledge field data of this type does not presently exist; therefore, we will utilize the laboratory data set of Haller et al. (2002). These data were collected in an 18 m x 18 m basin with a planar (1:30) beach. Three "sand bar" sections were emplaced on the slope leaving two gaps for rip channels as shown in Figure

2. Most of the data used in this paper consists of wave height and wave setup measurements made along two cross-shore transects. The first transects extends through the channel on the right-hand side of Figure 2, and the second crosses the middle of the center bar section. We also used cross-shore current measurements made along the channel transect. For the model/data comparisons we selected five wave conditions (tests B, C, D, E, and G), which consisted of monochromatic, normally incident waves. The time-averaged (~26 min) experimental parameters are listed in Table 1.

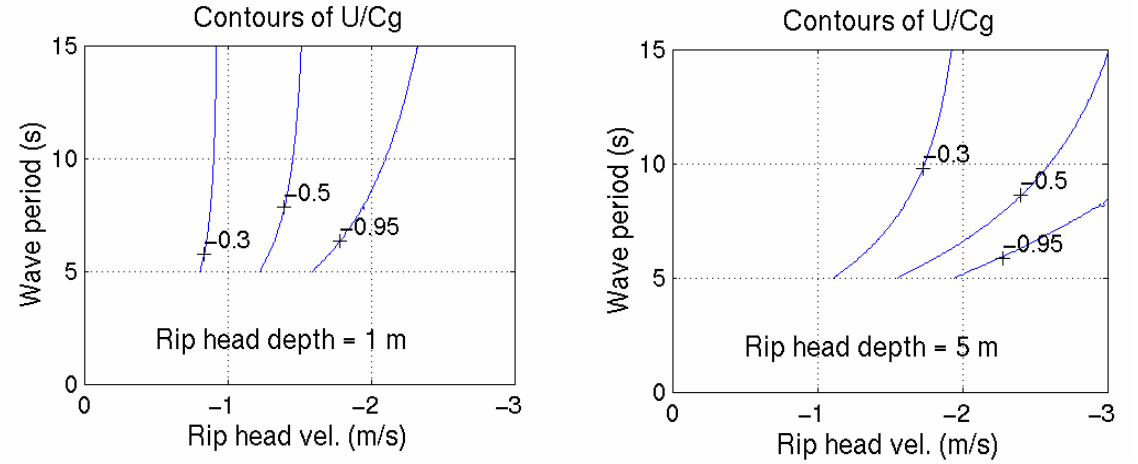

Figure 1: Contours of wave blocking parameter *U*/*Cg* for typical field-scale rip currents in water depths of (*left*) 1 m and (*right*) 5 m.

The prototype conditions for each test are plotted in Figure 3 along with the contours of *U*/*Cg*. The prototype conditions were calculated based on an undistorted Froude scaling of the experimental conditions with model/prototype length and time ratios of 1:50 and $1:(50)^{1/2}$, respectively. Based on this length scale ratio, the prototype depth at the rip current velocity maximum was approximately 5 m and the figure shows that, for tests B, C, E, and G, the waves near the rip are far from the blocking point, similar to most field conditions. However, wave blocking did occur during test D.

Bore Dissipation Models

Based on an analogy with dissipation in a turbulent bore (LeMéhauté, 1962), the dissipation in a breaking wave can be parameterized as follows:

$$D = -\frac{\beta}{8\pi}\rho g k H^3 \sqrt{\frac{g}{\zeta}}, \tag{4}$$

where β is a nondimensional dissipation coefficient, and ζ is a vertical length scale that, for depth-induced breaking, is commonly taken to be the local water depth h. The model of Battjes and Jansen (BJ) also simplifies Eq. 3 by assuming the breaking waves are in shallow water ($\omega/k = \sqrt{gh}$) and that $H/h \sim 1$. For strictly current-induced breaking, the CK model assumes $\zeta = k^{-1}\tanh(kh)$ for the vertical length scale. The advantage of this scaling is that it is better suited for intermediate and deep water breaking and reduces to $\zeta = h$ in shallow water. In order to maintain consistency in our comparisons between the BJ and CK models, we will consider the BJ model without explicitly assuming shallow water waves or $H/h \sim 1$, but with the local water depth as the vertical scale.

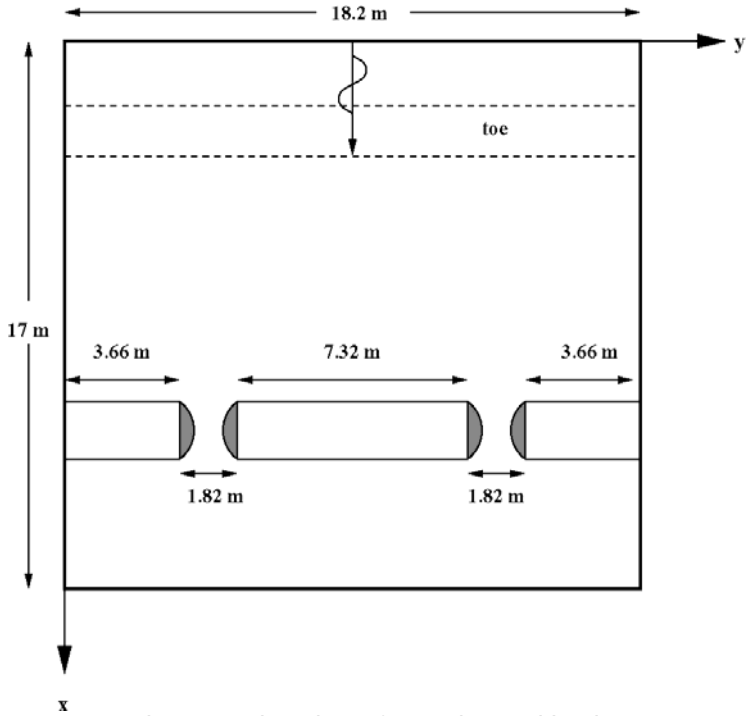

Figure 2: Plan view of experimental basin.

Table 1. Table of Experimental Conditions

Test	Maximum Rip Velocity (cm)	Deep Water Wave Height, (cm)	Wave Period, (sec)	Water Depth at Bar Crest, (cm)
E	-17.8	4.52	0.8	2.67
C	-26.2	5.22	1.0	2.67
D	-40.4	8.26	1.0	2.67
B	-20.9	5.12	1.0	4.73
G	-21.8	7.43	1.0	6.72

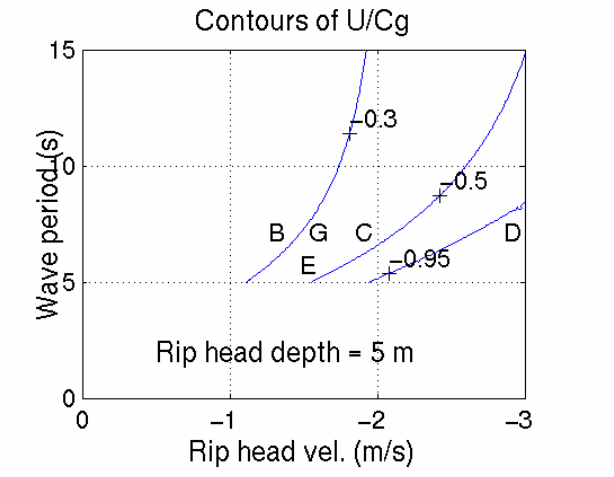

Figure 3: Prototype wave blocking conditions for experimental tests. Letters indicate the conditions during tests B, C, D, E, and G.

In order to integrate Eq. 1 using Eq. 3, several inputs are needed. First the total water depth (including the local setup/setdown) h is required as a function of cross-shore distance. Usually Eq. 1 is coupled with the cross-shore momentum balance, which governs the mean water level (i.e. the deviation of $h(x)$ from the still water level). However, in this work we are strictly interested in the modeling of wave dissipation near rip currents. Therefore, to remove any dependence of the results on the modeling of the cross-shore momentum balance, we will utilize the mean water level measurements to calculate $h(x)$ and input into the wave transformation model. In order to obtain $h(x)$ at the relatively fine cross-shore resolution necessary for the model, the data were linearly interpolated between the measurements.

In a similar fashion, the cross-shore velocity profile $U(x)$ is a required input to the model. For several of the tests the velocities were only measured at a few points in the channel; therefore, it was necessary to use a curve-fitting procedure to generate a finely-resolved current profile. The cross-shore profile of the rip current velocities were fit to a Gaussian curve given by the following:

$$U(x) = U_{\max}\, e^{-\frac{1}{2}\left(\frac{x-\mu}{\sigma}\right)^2}, \tag{5}$$

where $U_{\max}$ is the measured rip current maximum, μ is the cross-shore location of the rip maximum, and σ is a cross-shore length scale of the rip current profile. In order to fit this shape to the measurements, both μ and σ were allowed to vary and a 2-D parameter search was performed to find the best-fit current profile. The fitted current profiles are shown in Figures 4 and 5. The rip currents in tests B and C were best resolved by the measurements and Figure 4 shows that the measured profiles are well fit by the Gaussian shape. The current measurements in test B were the most extensive, and the secondary circulation that occurs shoreward of the base of the rip is evident as a shoreward flowing current in the region $x < 200$ cm. For this test, since the Gaussian curve goes to zero at locations far from the maximum, a linear correction was made to the calculated current profile in order to fit the measurements within the secondary circulation. In the other tests the velocity measurements did not resolve this secondary circulation, and no effort was made to account for it. This shoreward flowing current had a relatively small impact on the wave modeling in Test B, but should not be a factor in the other tests, since the wave transformation model was only carried forward to the most shoreward wave measurement (see wave and current measurements in Figures 4 and 5).

After calculating the cross-shore current and total water depth profiles and specifying the wave breaking dissipation formulation, the final two steps before Eq. 1 can be integrated in the shoreward direction are to specify the incipient breaking condition and the dissipation coefficient, β. For incipient breaking, the BJ model incorporates a modified version of the steepness-based criterion of Miche (1951), while the CK model uses the original Miche criterion given by:

$$H_b = \gamma \frac{\tanh kh}{k}, \tag{6}$$

where H_b is the wave height at the break point and γ is an empirical constant. In the original formulation $\gamma = 0.89$. The dissipation coefficient β is typically taken to be equal to 1.0. However, CK calibrated both γ and β for current-induced breaking.

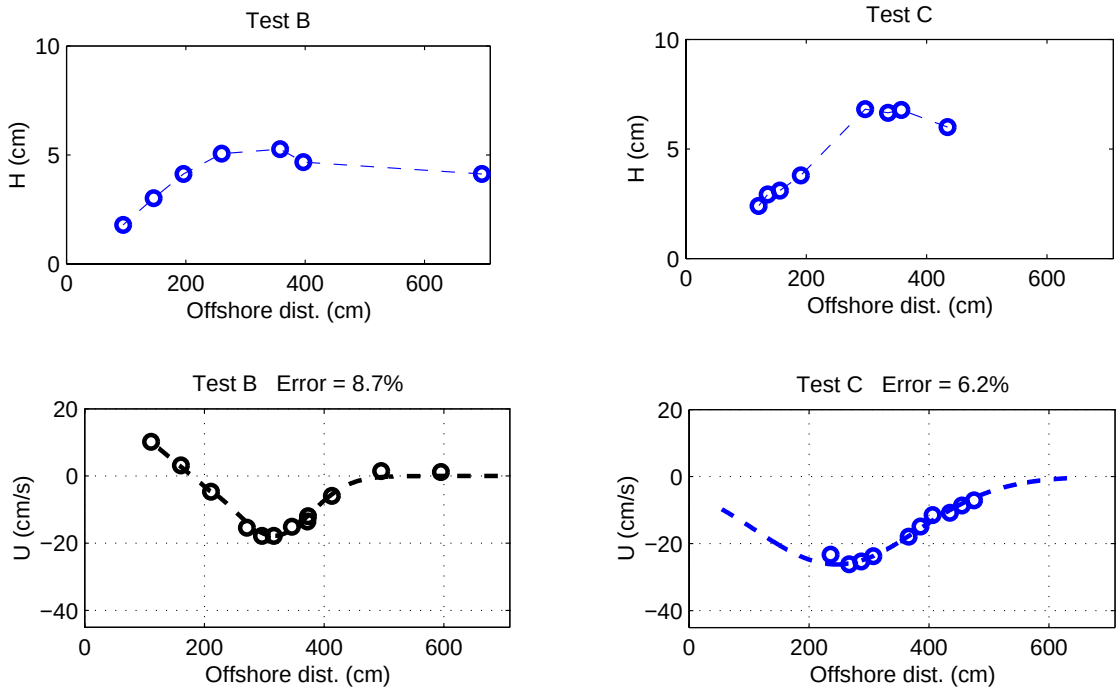

Figure 4: Measured wave height vs. cross-shore distance in rip channel (circle-dash, upper panels). Cross-shore velocity in rip channel (circles, lower panels). Gaussian fit to velocity measurements (dashed line, lower panels).

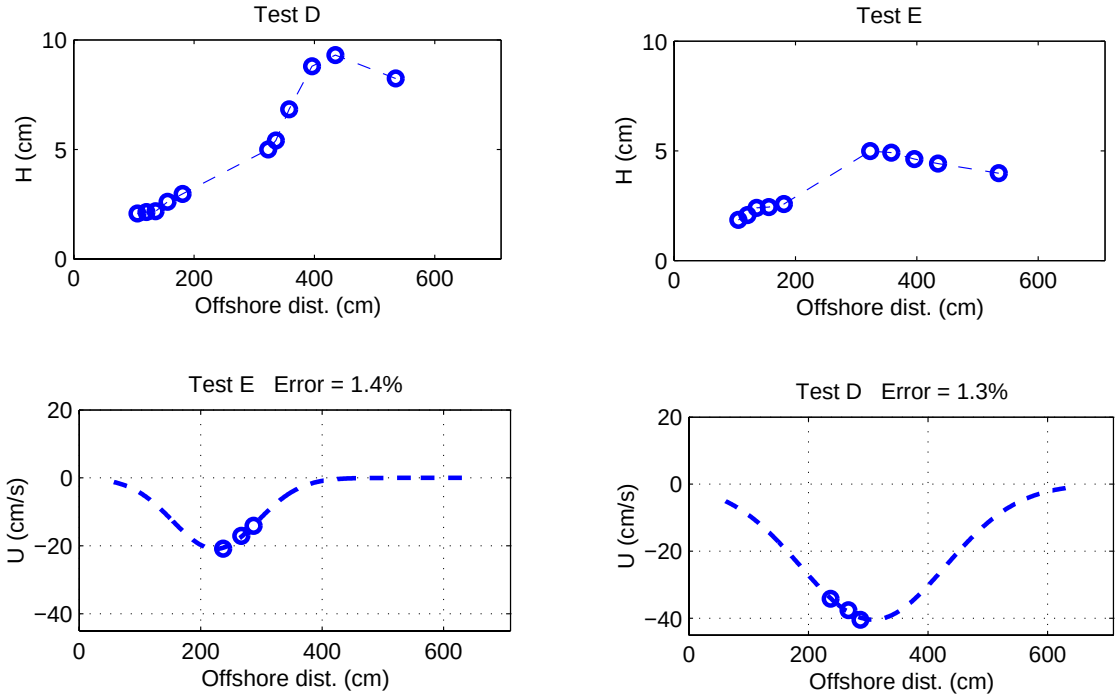

Figure 5: Measured wave height vs. cross-shore distance in rip channel (circle-dash, upper panels). Cross-shore velocity in rip channel (circles, lower panels). Gaussian fit to velocity measurements (dashed line, lower panels). Test G results are similar but omitted for brevity.

In order to examine the capabilities of the bore dissipation formulation for the modeling of wave dissipation near rip currents, we integrate Eq. 1 in the shoreward direction starting from offshore conditions and using Eq. 6 as the incipient breaking condition for both models. Modeled wave heights were compared to the measured wave heights along a cross-shore transect running through the rip channel and the rms error was calculated. For each test, the integration was carried out a large number of times in order to perform the 2-D search for the best-fit values of β and γ. The purpose was to determine whether these models can effectively simulate the combined depth- and current-induced breaking that occurs near rips if we allow for tuning of the coefficients and then to compare the tuned coefficients to the values found by BJ and CK.

The CK model results for the waves in the rip channel are shown as dashed lines in Figure 6. The results from the BJ model are not shown because, using their respective best-fit coefficients for each test, the results from the two bore dissipation models are indistinguishable from each other. One might conclude that this results from the wave breaking occurring in shallow water, which would eliminate the differences between the vertical scales in the two models. But this is not the case, in fact, the waves start to break in intermediate depths ($kh \approx 1$); if the breaking waves had been in shallow water the best-fit coefficients (listed in Table 2) would be exactly the same for these two models. Nonetheless, the coefficients for each model are very similar because, for the tested conditions, the models are relatively insensitive to the choice of vertical scale. On the other hand, making the explicit assumption that the breaking waves are in shallow water (as in the original BJ model) would significantly alter the calibrated values of the coefficients.

It is further evident from Figure 6 that, when calibrated, the models fit the data well. For example, the shoaling that occurs as the waves propagate towards the rip maximum is well predicted. In addition, the dynamics shoreward of the rip maximum are fairly complex, as the wave decay in this region results from some combination of de-shoaling, current-induced, and depth-induced breaking. Yet, the models do a fairly good job in this region also. Although, the results from test B show that the bore dissipation models would prefer to break the waves significantly shoreward (x=200 cm) of what is shown by the measurements (x=250 cm) and confirmed by visual observations.

As a final note, the onset of rapid oscillations shoreward of the break point in test D, are a manifestation of wave blocking on the rip. The blocking point predicted by linear theory appears to correspond to the observed steep decline in the wave height data. Although, it should be noted that the measured wave heights do not go to zero in the blocked region owing to 2-D effects, as energy must naturally diffract into the wave blocking region.

The most significant result of the model/data comparisons is that the best-fit coefficients are very different from what has been found for strictly depth-induced breaking. Using a large data set from both lab and field experiments and barred and planar beaches, Battjes and Stive (1985) calibrated the BJ model and developed an empirical formula for calculating γ a priori based on the offshore wave steepness. When applied to these rip current experiments their formula recommends a range of $0.80 < \gamma < 0.88$; in addition, the BJ model assumes β=1.0. In contrast, CK calibrated γ and β using measurements of strictly current-induced breaking and they determined that the optimal values were 0.6 and 0.1,

respectively. This suggests that wave breaking on opposing currents occurs at lower steepness and the dissipation occurs at a slower rate than for depth-induced breaking. Correspondingly, the best fit values for wave breaking on rip currents, where both depth- and current-induced breaking occurs, lie in between the strictly depth- or current-induced cases and rather close to the current-induced values of CK. However, 2-D effects would be largest for test D, since the waves are highly nonlinear and the rip current is quite strong.

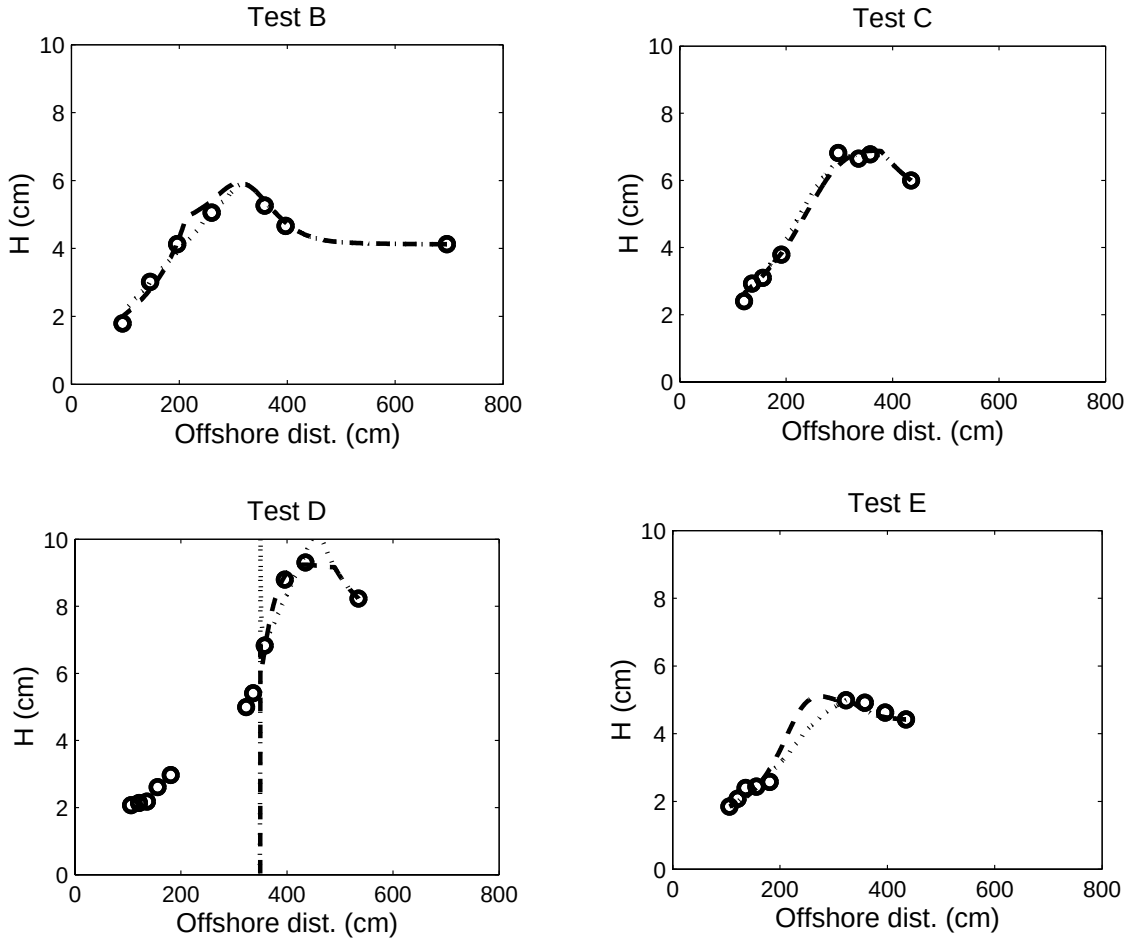

Figure 6: Wave height vs. cross-shore distance along a transect through the rip channel for CK model (dashed) and DDD model (dotted). Measured wave heights shows as circles. Best-fit coefficients are listed in Table 2. Model results for test G omitted for brevity.

Table 2. Best-fit (rms error ~ 4.5%) bore dissipation coefficients for waves in rip channel.

Test	γ_{BJ}	γ_{CK}	β_{BJ}	β_{CK}
Mean	0.68	0.67	0.37	0.33
Std. Dev.	0.07	0.06	0.30	0.30

As a control test on the modeling, the same comparisons were made for the waves propagating over the bars where the offshore currents are small. For brevity the modeled wave transformation is not shown here but the calibrated constants are shown in Table 3. Clearly, the values of β are significantly larger and closer to what we would expect for depth-induced breaking. It also should be noted that the barred bathymetry with

monochromatic waves is particularly difficult for these models, since they do not contain a mechanism for allowing the waves to cease breaking.

Table 3. Best-fit (rms error ~ 5.6%) bore dissipation coefficients for waves over bar.

Test	γ_{BJ}	γ_{CK}	β_{BJ}	β_{CK}
Mean	0.63	0.63	0.72	0.69
Std. Dev.	0.14	0.14	0.19	0.19

Stable Energy Flux Model

The dissipation model of Dally, Dean, and Dalrymple (1986; hereinafter DDD) is based on the heuristic assumption that waves have an underlying "stable" energy flux, such that the waves will cease breaking when the energy flux has been reduced to the locally stable value. Hence, the model does particularly well with barred beaches, where breaking often ceases in the bar trough region. They parameterize the wave dissipation by the following:

$$D = -\frac{\mathrm{K}}{h}\left[ECg - E_s Cg\right], \tag{7}$$

where K is a dimensionless decay coefficient, ECg is the local energy flux, and E_sCg is the local stable energy flux defined as $E_s=\rho g H_s^2/8$. Thus, E_s is associated with the stable wave height H_s, defined as $H_s=\Gamma h$. In their model/data comparisons DDD did not consider the effect of the incipient breaking condition, but simply concentrated on modeling the wave transformation once wave breaking had commenced. However, in order to effectively evaluate the DDD model for simulating wave breaking near rips we need to specify an incipient breaking condition. Therefore, we will again employ the Miche criterion with γ allowed to be a free parameter. In addition, we again have a dissipation coefficient, K, and a new coefficient, Γ, which governs the cessation of breaking and also influences the rate of wave decay.

In a similar fashion to the bore dissipation models a parameter search (in 3-D) was performed and the best-fit coefficients were determined. The model/data comparisons for the tuned coefficients are shown in Figure 6 as dotted lines. Again, the model/data agreement is quite good with the rms errors slightly smaller for the DDD model than for the bore dissipation models, but the difference is probably not statistically significant. In addition, the DDD model does not require the waves in test B to start breaking too far shoreward as did the BJ and CK models.

Again, it is of interest to compare the tuned coefficients for the rip current cases to previously found values. DDD calibrated their model with laboratory data obtained on planar beaches and suggest the following values for a planar beach with 1/30 slope: K=0.275, Γ=0.475, and γ=0.89 (Miche). The coefficient that give the best model/data fit for waves propagating up the plane slope through the rip channel are listed in Table 4. The mean values for the set of experiments are not drastically different from the suggested values of DDD, however, the range of K values determined for the individual tests is quite large. This is a result of the lack of sensitivity of the DDD model to K when the incipient breaking is added as a free parameter. Essentially, these three parameters are not completely independent. In summary, the DDD model can be fit to the data quite well,

however, it would appear difficult to use the model in a predictive sense (*i.e.* specify the coefficients a priori) for wave transformation near rip currents.

The 3-D parameter search was also performed for the waves propagating over the bar. The best-fit values are listed in Table 5. As expected, the DDD model does quite well for this case. In addition, the variability of the coefficients for different tests is much reduced and the mean values are closer to the suggested values.

Table 4. Best-fit (rms error ~ 3.9%) DDD model coefficients for waves in rip channel.

Test	γ_{DDD}	K_{DDD}	Γ_{DDD}
Mean	0.70	0.34	0.38
Std. Dev.	0.12	0.30	0.38

Table 5. Best-fit (rms error ~ 2.3%) DDD model coefficients for waves over bar.

Test	γ_{DDD}	K_{DDD}	Γ_{DDD}
Mean	0.73	0.28	0.38
Std. Dev.	0.10	0.06	0.13

IMPACT ON NEARSHORE DYNAMICS

In order to assess the importance of the modeling of wave dissipation on rips to the overall driving of the nearshore circulation, we calculate the impact of the various dissipation models on the generation of the longshore pressure gradient that drives the rip circulation. In the simplest sense, the cross-shore momentum equation is given by:

$$\frac{\partial \bar{\eta}}{\partial x} = \frac{1}{\rho g h}\frac{\partial S_{xx}}{\partial x}, \tag{8}$$

where $\bar{\eta}$ is the mean water level and S_{xx} is the cross-shore component of the radiation stress. Based on linear theory, S_{xx} is given by:

$$S_{xx} = \frac{1}{8}\rho g H^2 [2n - \frac{1}{2}], \tag{9}$$

.

In Eq's. 5 and 6 we have neglected the effects of bottom friction and wave rollers. This is so that we can isolate the effect of the longshore variability in the wave breaking dynamics on the model predictions of the longshore setup gradient. For example, when using nearshore wave and current models in a predictive sense or to investigate nearshore dynamics, the typical scenario would be to calibrate the wave propagation model based on steady conditions (barred or planar) in the absence of highly transient rip currents. However, when the models are applied to (or predict) the case when rip currents are present the results of the previous sections would indicate that the empirical coefficients contained in the wave transformation models and tuned for the depth-induced breaking will be far from optimal for the accurate modeling of the combined depth- and current-induced breaking that occurs near rip currents. In other words the optimal coefficient values for the wave modeling vary in the longshore direction and this has some unforeseen impact on the accuracy of the simulated nearshore dynamics.

In order to investigate the impact of less –than-optimal coefficient values on the driving of rip current circulation, we consider two scenarios, the first being that the wave model is optimized for simulating the waves over the bars and then used to predict the wave transformation and setup in the channel. The impact on the driving of the nearshore currents is assessed by calculating a proxy for the longshore pressure gradient, which is simply $\overline{\eta}_{bar}(x) - \overline{\eta}_{chan}(x)$, and comparing that to the "ground truth" value that would be given by optimizing the wave transformation for the bar and channel transects individually. The second scenario uses a global optimization of the empirical coefficients in the wave modeling. The global optimization involved performing the coefficient calibration where the model/data errors in the channel and over the bar were equally weighted. Thus, the best fit values were those where both transects were modeled equally well.

Figure 7 shows the effect of the different coefficient optimizations on the modeling of the wave transformation and the predicted setup in the surf zone for test B. Since the DDD model gave arguably the best model/data agreement for both the bar and channel transects, this is the only model considered for this aspect of the study. The figure shows that using the bar optimized parameters for the modeling of the waves in the channel leads to significant discrepancies in the wave height and setup predictions. The global optimized parameters do a better job in the channel, although the wave breaking begins well shoreward of what was observed. However, it should be noted that the bar optimization scheme is by far the likely scenario in practice, since field data regarding wave transformation in the rip channel are nonexistent at this time.

It is also interesting to note that the model can still do a fair job over the bar with the global optimized values. This is because the shallow depth at the bar crest exerts a fairly strong control on the wave decay, hence the model is less sensitive to the coefficient values. Figure 8 compares the net mean water level difference between the channel and bar transects based on the different optimizations. The figure indicates that the difference between the bar optimized and ground truth scenarios can be quite large. For example, the maximum pressure gradient is 40-50% larger in the ground truth profile than in the bar optimized profile. The global optimized profile is closer to the ground truth but some differences still exist.

CONCLUSIONS

A modeling exercise was performed using the wave action balance equation including wave breaking dissipation with different parameterizations in order to evaluate the ability of several existing models to simulate the combined depth- and current-induced breaking that occurs near rip currents. Model results were compared with existing laboratory data and model coefficients were calibrated for the cases of waves propagating on rips and for waves propagating over a longshore bar in the absence of currents.

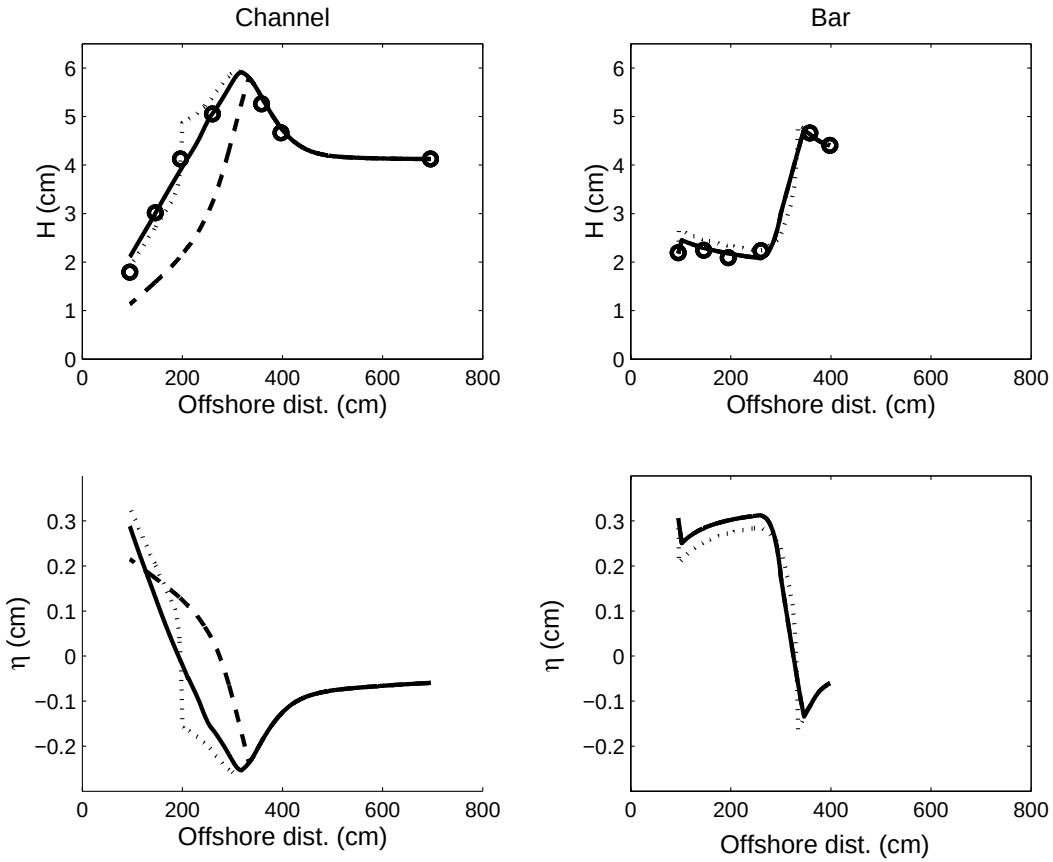

Figure 7: Modeled wave height and MWL using “ground truth” optimization (solid), bar optimization (dashed; dashed and solid lines lie on top of each other for bar transect), and global optimization (dotted). Measured wave heigts shown as circles.

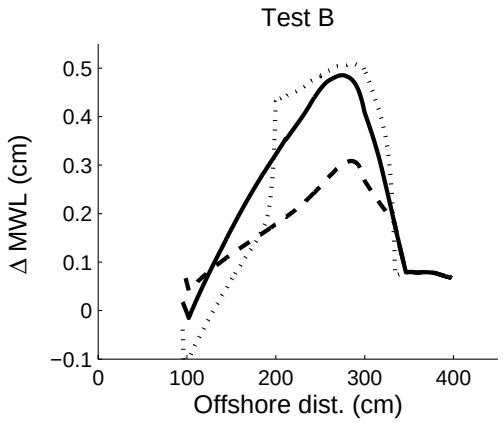

Figure 8: Cross-shore profile of the net difference in the mean water level between the bar and channel transects using “ground truth” optimization (solid), bar optimization (dashed), and global optimization (dotted).

The bore dissipation models of BJ and CK and the stable energy flux model of DDD all fit the data well when the coefficients were calibrated for individual tests. Both the BJ and CK models gave very similar results, which indicates that the results were not sensitive to the specification of the vertical length scale in the bore dissipation parameterization. However, the calibrated coefficients for the wave transformation in the rip channel were similar to those found by CK for strictly current-induced breaking. This suggests the importance of current-induced breaking on rip currents and highlights the difficulties in using depth-induced breaking models for predicting wave decay near rips.

The impact of using less than optimal model coefficients in the modeling of wave decay near rip currents and the resulting longshore pressure gradients that are linked to this wave decay were analyzed. The results suggest that wave transformation is likely to be poorly modeled near rip currents. Employing a simplified cross-shore momentum balance it was shown that the wave setup is, therefore, also poorly predicted and hence the longshore pressure gradients will suffer from the same effect. The wave transformation over the bar was less sensitive to the model coefficients, which also implies that the wave transformation in the channel is the controlling factor in the driving of the nearshore currents due to longshore pressure gradients. Or in other words, it is fairly straightforward to model the dynamics over the bars, but simulating what is happening in the rip channel is trickier and the nearshore circulation is highly sensitive to the channel dynamics, at least for the conditions considered here.

Finally, the importance of wave blocking due to rip currents was assessed using linear wave theory. Based on a range of typical wave and current scales observed in the field, it was found that wave blocking by rips requires rip velocities in excess of 2 m/s and wave periods of less than 8 sec. This suggests that wave blocking by rips should be fairly rare.

REFERENCES

Battjes, J.A. and Janssen, J.P.F.M. 1978. Energy loss and set-up due to breaking of random waves, *Proc. of the 16th Intl. Conf. on Coast. Eng.*, ASCE, 569-587.

Battjes, J.A. and M.J.F. Stive 1985. Calibration and verification of a dissipation model for random breaking waves, *J. Geophys. Res.*, *90*, C5, 9159—9167.

Chawla, A. and Kirby, J.T. 2002. Monochromatic and random wave breaking at blocking points, *J. Geophys. Res.*, *107*, C7, 10.1029/2001JC001042.

Dally, W.R., Dean, R.G., and Dalrymple, R.A. 1985. Wave height variation across beaches with an arbitrary profile, *J. Geophys. Res.*, *90*, C6, 11,917—11,927.

Haller, M.C., Dalrymple, R.A., and Svendsen, I.A. 2002. Experimental study of nearshore dynamics on a barred beach with rip channels, *J. Geophys. Res*., *107*, C6, 10.1029/2001JC000955.

LeMéhauté, B. 1962. On non-saturated breakers and the wave run-up, *Proc. 8th Int. Conf. Coast. Eng.*, ASCE, 77—92.

Miche, M. 1951. Le pouvoir reflechissant des ouvrages maritimes exposes a l'action de la houle, *Annals des Ponts et Chausses*, 121e Annee, 285—319, (translated by Lincoln and Chevron, University of California, Berkeley, Wave Research Laboratory, Series 3, Issue 363, June 1954).

KEYWORDS – ICCE 2002

WAVE BREAKING AND RIP CURRENT CIRCULATION

Merrick C. Haller and H. Tuba Özkan-Haller

Rip currents
Breaking waves
Wave-current interaction
Nearshore circulation
Wave modeling